Indian Geotechnical Journal, 34 (2), 2004

Engineering Behaviour of Jointed Rock Mass

Mahendra Singh*, K.S. Rao† and T. Ramamurthy‡

Introduction

Many important engineering structures e.g. dam, tunnel, bridge pier, cavern for hydroelectric scheme or repository for radioactive waste disposal are built on and in rock masses. Insitu stresses, pore water pressure, rock mass strength and deformation modulus are the most common input parameters needed for design of these structures. The present paper deals with the last two parameters i.e. rock mass strength and deformation modulus of the rock mass.

The rock masses encountered in the field are invariably discontinuous. Joints are the most common discontinuities. Their presence reduces the strength and increases the deformability of the mass. They also render anisotropic behaviour in strength and deformability of the mass. The relative scale of excavation or extent of foundation with respect to the spacing and number of discontinuities decide if the rock mass should be treated isotropic or anisotropic. For isotropic mass, theories developed by Hoek and Brown (Hoek, 2000) may be used to assess the rock mass strength. For anisotropic masses, the use of these theories is not recommended (Hoek, 2000). The present study basically deals with the assessment of the engineering properties of an anisotropic rock mass. However, the method may be used for isotropic rock mass as well.

Numerical modelling of discontinuities is a powerful tool for designing

* Associate Professor, Civil Engineering Department, IIT Roorkee, Roorkee – 247667, UA, India.

† Associate Professor, Civil Engineering Department, IIT Delhi, New Delhi – 110016, India.

‡ Retd. Professor, Civil Engineering Department, IIT Delhi, New Delhi – 110016, India.

underground excavations and support structures especially at the detailed design stage and also during construction. However, the quantity and quality of input data required by these sophisticated techniques limit significantly the practical use of these approaches; since, with the conventional site investigation means it is practically impossible to know beforehand the characteristics of discontinuities required for modelling (Xu et al., 2003). In the preliminary stages of the projects, the relatively less sophisticated techniques e.g. RMR (Bieniawski, 1973 and 1989), RSR (Wickham et al., 1972) and Q (Barton et al., 1974) are more popular. These techniques treat the discontinuous rock mass as a continuous material that has properties equivalent to the discontinuous medium.

The concept of Joint Factor proposed by Ramamurthy and co-workers (Ramamurthy, 1993; Ramamurthy and Arora, 1994) also falls in the category of equivalent material approach. The concept was developed on the basis of experimental studies conducted on cylindrical specimens (76 mm height, 38 mm diameter) of intact and jointed rocks (Arora, 1987; Roy, 1993). In field, however, the anisotropic rock mass generally consists of blocks of intact rock material separated by discontinuities. A blocky mass has more freedom for movement of the blocks, which affects the failure mechanism and the response of a blocky mass is different from the rock intersected by a single joint. Also, the problem of scale effect cannot be ruled out from results on small cylindrical specimens. It was therefore decided to validate the Joint Factor concept for jointed anisotropic block mass. The following were the main objectives of the study:

i. To carry out experimental investigation on large sized specimens of jointed block mass. The specimens should have sufficient number of blocks so to have minimum or no scale effect. Previous experience (Walker, 1971; Lama, 1974) indicates that if there are about five elemental blocks in any direction, the asymptotic value of the property is reached.

ii. To capture the effect of variation in configuration of joints i.e. their orientation, frequency and interlocking condition.

iii. To validate the applicability of Joint Factor concept to jointed block mass by suitably modifying it and thus establish a link between the strength and modulus values of intact rock and jointed block mass through Joint Factor.

Experimental Programme

In rock mechanics literature, physical model tests have been used extensively to understand the mechanism of failure of jointed rock masses.

Some of the previous studies through physical models on jointed rocks are those by Goldstein et al. (1966), Hayashi (1966), Brown (1970a, 1970b), Brown and Trollope (1970), Walker (1971), Ladanyi and Archambault (1972), Einstein and Hirschfeld (1973), Lama (1974), Baoshu et al. (1986) and Yang and Huang (1995). Model materials have been used in these studies to simulate the rock material mainly due to the following two reasons:

i. It is relatively easy to work with model material and create the discontinuities at desired configuration.

ii. Reproducibility of results is much higher for model materials as they are manufactured under controlled conditions. The natural rock, which forms under natural uncontrolled environment, is expected have high scatter in results (Abdullah and Dhawan, 2003). It was therefore decided to use a suitable model material to simulate the intact rock in the present investigation.

A review of the previous studies indicates that most of these studies were directed towards understanding the behaviour of jointed rock under confined state. It should be noted that the effect of the discontinuities on the strength and deformation of the mass is maximum when the normal stress on the discontinuity surface is very low. Since, the objective of this study has been to study the effect of joints and their configuration, it was decided that experiments be conducted under uniaxial compression condition (Singh, 1997; Singh et al., 2002). Practically, uniaxial loading conditions are nearly applicable for foundations at shallow depth and walls of underground openings after excavation. Also, the uniaxial compressive strength (UCS) of the mass provides the lower limit for the confined strength and used as an input parameter in strength criterion (Ramamurthy, 1993; Ramamurthy and Arora, 1994). If reasonably good estimates could be made on this lower limit, the predicted confined strength may be expected to be accurate.

Model Material

After making trials for several materials, commercially available sand-lime bricks (23 × 10 × 7 cm) were selected as the model material. The bricks were bought from M/s. U.P. Mineral Products Ltd., Village Palli, Baghpat, Meerut, U.P. To manufacture the bricks, sieved sand was mixed with lime and water with hardness less than 350 ppm. The mixture was poured into dies and pressed at a pressure of about 39.6 MPa. Autoclaving of the prepared moulds was done for 4 hours at 180°C and afterwards the bricks were cured in air for about three weeks.

The material has a uniaxial compressive strength (UCS) of 17.13 MPa and represents a weak rock classified as "EM" on Deere-Miller (1966)

TABLE 1 : Engineering and Physical Properties of the Model Material

Property	Value
Dry density, γ_d (kN/m^3)	16.86
Porosity (%)	36.94
UCS, σ_{ci} (MPa)	17.13
Brazilian strength, σ_{ti} (MPa)	2.49
Tangent modulus, E_i (GPa)	5.34
Poisson's ratio, ν_i	0.19
Cohesion, c_i (MPa)	4.67
Friction angle of intact material, ϕ_i^o	33.00
Friction angle along the joints, ϕ_j^o	37.00
Deere-Miller classification (1966)	EM

classification chart. The physical and engineering properties of the model material were obtained as per the suggested methods of ISRM (1981); the tests for engineering properties, were however, performed on cylindrical cores of 38 mm diameter with appropriate height to diameter ratio. The shear strength parameters of the intact material were computed by performing triaxial tests with confining pressure equal to 0.98, 1.82, 2.89 and 4.07 MPa. The value of friction angle, ϕ_j for the block joints was computed by conducting direct shear tests on joint surface between two blocks of size 5.92 cm × 5.92 × 2 cm each. The tests were performed under low normal stress (upto a maximum σ_n = 0.30 MPa). To maintain uniformity in the material forming the jointed specimens, the cubes of the material were tested for UCS prior to forming the specimens. The physical and engineering properties of the model material are presented in Table 1.

Preparation of Specimens

The brick was first cut into slices of 2.5 cm thickness; these slices were cut into prismatic bars, which were further cut into cubes of 2.5 cm side (Fig.1). The cubes and prismatic bars were arranged in certain fashion and cut to get the desired configuration of joints (Fig.2). These cut blocks were arranged to form the specimen of jointed block (Fig.3). The assembled specimens could be grouped into four categories i.e. A, B, C and D.

The first category of the assembled specimens, termed Type-A, consists of the cubical elemental blocks of 2.5 cm side, arranged in such a manner as to form three sets of the joints. To have a reasonably scale free jointed

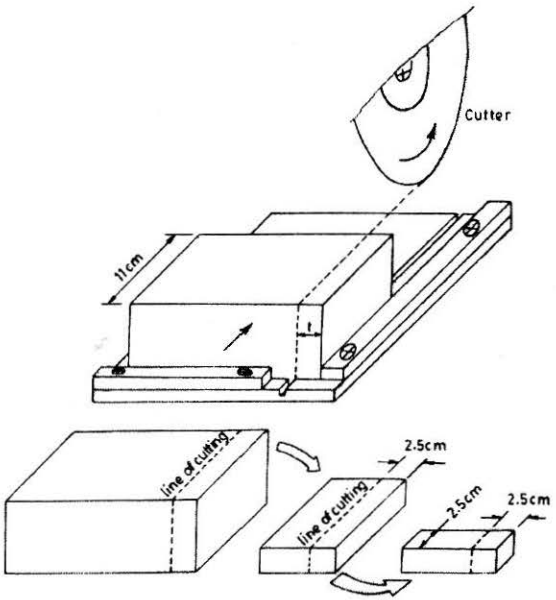

FIGURE 1 : Arrangement for Cutting Bricks into Smaller Blocks

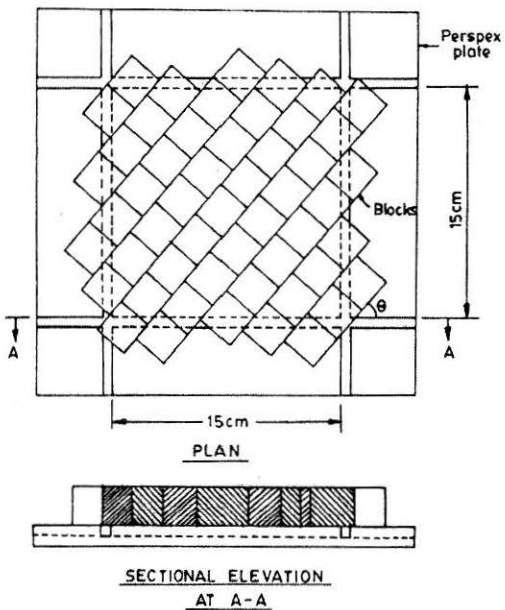

FIGURE 2 : Plan and Front View (Sectional) of Blocks Arranged to be Cut for Desired Configuration

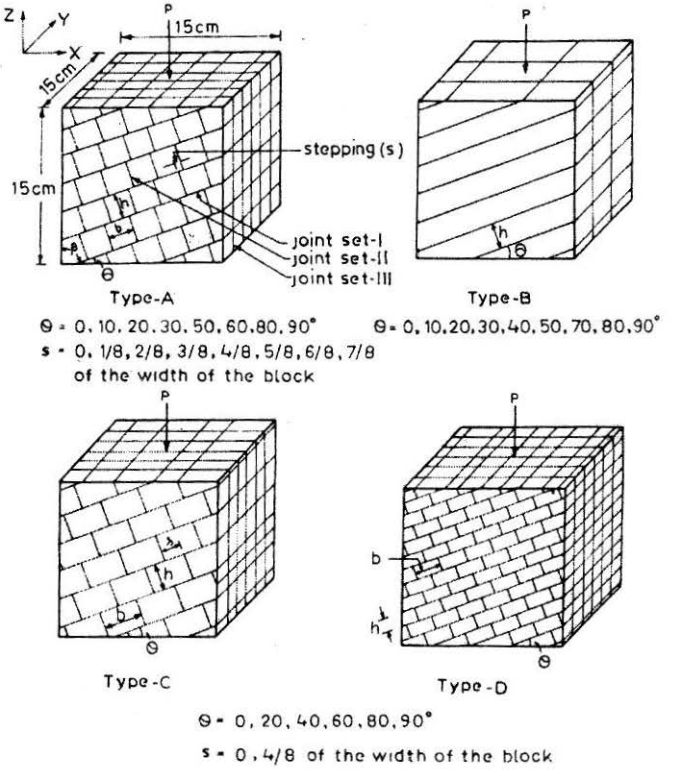

FIGURE 3 : Configurations of Joints Tested

block mass, it was decided to have at least six elemental blocks in each direction. The size of each specimen was 15 × 15 × 15 cm and on an average, it consisted of more than 260 elemental blocks. The joints in Set-I were continuous and orientated at a variable inclination θ (Fig.3). The values of θ adopted were 0, 10, 20, 30, 50, 60, 80 and 90° respectively. The joints in Set-II were stepped at variable stepping, 's'. For each orientation θ, the values of s were 0, 1/8, 2/8, 3/8, 4/8, 5/8, 6/8, 7/8 of the width of the element block respectively. The joints in Set-III remained vertical.

The specimens of Types-B, C and D were formed by changing geometry of the elemental blocks. In Type-B, plates of 2.5 cm thickness were used. The values of θ adopted for type-B were 0, 10, 20, 30, 40, 50, 70, 80 and 90° respectively. For Type-C, the elemental block had a block width, b = 3.75 cm and block height, h = 2.5 cm. For Type-D, these dimensions were 2.5 and 1.25 cm respectively. The details of geometry of the elemental blocks are presented in Table 2.

TABLE 2 : Details of Elemental Block Geometry in Test Specimens

Specimen Type	Dimension of Elemental Block		Inclination ($\theta°$)	Stepping
	Width b (cm)	Height h (cm)		
A	2.5	2.5	0, 10, 20, 30, 50, 60, 80 and 90°	0, 1/8, 2/8, 3/8, 4/8, 5/8, 6/8 and 7/8 of the width of block
B	Extending full width of test specimen	2.5	0, 10, 20, 30, 40, 50, 70, 80 and 90°	
C	3.75	2.5	0, 20, 40, 60, 80 and 90°	0, 4/8 of the width of elemental block
D	2.5	1.25	0, 20, 40, 60, 80 and 90°	0 and 4/8 of the width of the block

Testing of Specimens

The jointed specimens (Types-A, B, C and D) were tested under uniaxial loading condition by applying a uniformly distributed load on the top surface. To minimize end friction, two sandwiches of Teflon sheets, smeared with silicon grease, were used at the top and the bottom of the specimen. LVDTs were used to measure deformations of all the six faces of the test specimen. The load was applied through a strain controlled loading arrangement. The rate of deformation was so adjusted that the failure took place within about 15 to 20 minutes of start of the experiment. The deformations were continued till the load, after failure, decreased to about half to one third of its peak value. The mode initiating the failure was recorded. The specimens were photographed after the experiment was over.

Results and Discussion

The axial stress, at any instant, was computed by dividing the load by the corrected area of the specimen. The axial strain, ε_z and the transverse strain, ε_x were computed as the ratio of change in the respective dimension of the specimen to the original dimension. The compressive stress and strains are considered positive. The results were plotted in the form of stress-strain curves. Some of the typical stress curves are presented in Fig.4. The

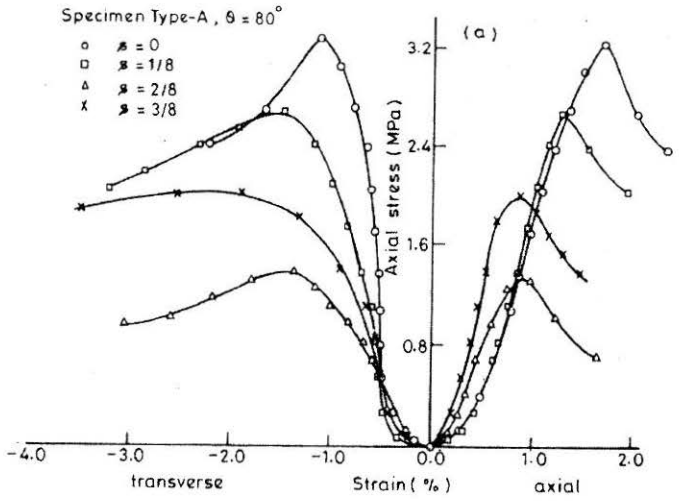

FIGURE 4 : A Few Typical Stress Strain Curves

transverse strain, ε_x is generally negative. The curves showing variation of axial stress with axial strain are generally non linear and S-shaped. Near the origin, the curve is concave upward, which indicates closure of joints and initial seating effect. The middle portion of the curve is linear that exhibits elastic deformations. Near failure, the curve becomes concave downward, exhibiting plastic deformations. The gradient of the middle linear portion of the curve was measured and termed as Tangent Modulus, E_j. In general, a tangent was drawn to the axial stress-axial strain curve at 50% of the peak stress to determine the tangent modulus. The peak stress from the stress-strain curve is considered as the uniaxial compressive strength (UCS) of the jointed mass for the particular joint configuration.

Strength Behaviour

One of the most important features of the joints is that they introduce anisotropy in engineering properties i.e. strength and deformability of the rocks. The anisotropy curve (Singh et al., 1989; Ramamurthy, 1993) represents the variation of strength of the mass with angle β, where β is the angle between the plane of discontinuity and stress direction. On basis of the anisotropy curve, Singh et al. (1989) have classified the strength anisotropy as U-type and undulatory type. The results on strength of the test specimens were plotted against angle, β as shown in Figs.5a and 5b. The angle, β has been taken as the angle of continuous joint plane (Set-I) with the direction of loading. The strength is shown in the form of a dimensionless ratio, σ_{cr}, which is defined as:

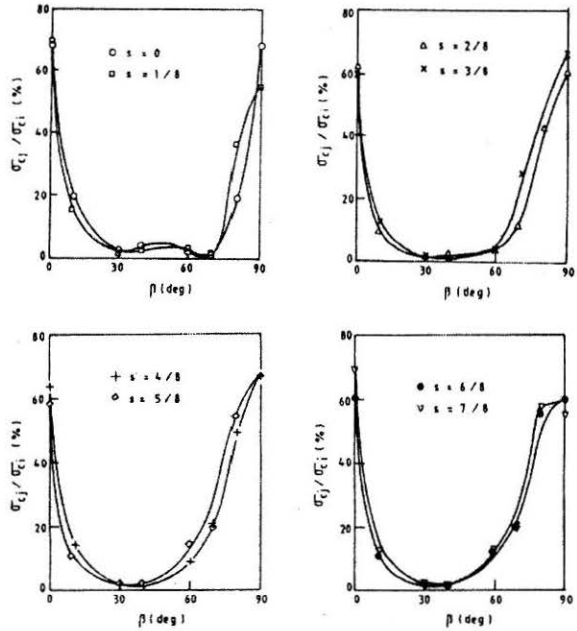

FIGURE 5a : Anisotropy in Strength Behaviour (Type-A Specimens)

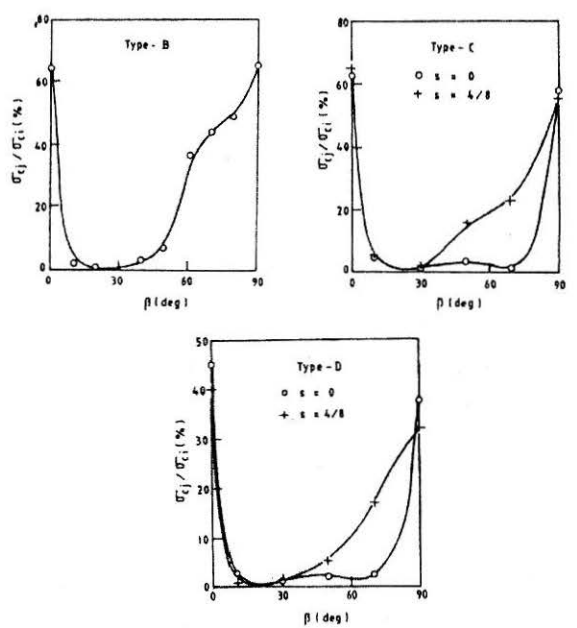

FIGURE 5b : Anisotropy in Strength Behaviour (Type-B, C and D Specimens)

$$\sigma_{cr} = \frac{\sigma_{cj}}{\sigma_{ci}} \tag{1}$$

where σ_{cr} = strength ratio,

σ_{cj} = UCS of jointed block mass,

σ_{ci} = UCS of intact model material.

It has been observed from Fig.5 that the block mass behaves highly anisotropically in strength behaviour. For Type-A and s = 0, the strength was about 68% at $\beta = 0°$ and dropped sharply to about 3% at $\beta = 30°$. A small increase was observed at $\beta = 40°$, beyond which, again the strength continues to be very low till $\beta = 70°$, beyond which there was a steep rise in the strength. A U-shaped anisotropy curve with very vide base, unlike the undulatory type for jointed rock as suggested by Singh et al. (1989), was obtained. As stepping increases the shape of the anisotropy curve remains almost same for $\beta < 30°$. However, for higher stepping, there is some enhancement in the strength values for $\beta > 40°$, due to which the shape of the anisotropy curve shifts little towards undulatory type. It may be concluded that the interlocking generated by higher stepping, induces enhancement in the strength for $\beta > 40°$ (sub horizontal joints). For $\beta < 30°$ (sub vertical joints), the interlocking generated by stepping does not provide any strength enhancement. A possible reason for this could be as follows:

If the friction angle of the jointed mass is ϕ_m, the mass will have minimum shear strength along a potential failure plane oriented at an angle $(45° - \phi_m/2)$ with the loading direction. If any of the joint planes is favourably inclined at this orientation, sliding will take place on this critical joint plane. If the continuous joint set is oriented in such a manner that β is close to $(45° - \phi_m/2)$, sliding will take place easily and the mass will offer very little resistance i.e. strength will be low. However, if the joint Set-II is close to $(45° - \phi_m/2)$ and stepping is large, the potential failure plane will have to shear the intact material as the joint is not continuous. The jointed mass will therefore offer higher resistance to failure. For example, if a typical value of ϕ_m is assumed $\approx 30°$, it can be seen that for joint Set-I oriented near $\beta \approx 30°$, no strength enhancement will take place due to interlocking introduced by stepping. This is why the strength obtained for these orientations is very low.

Deformational Behaviour

Besides strength, deformation of stressed rock mass is another important parameter. The tangent modulus, E_j gives an idea of the deformability of the mass. Higher the value of E_j, lower will be the deformability of the mass.

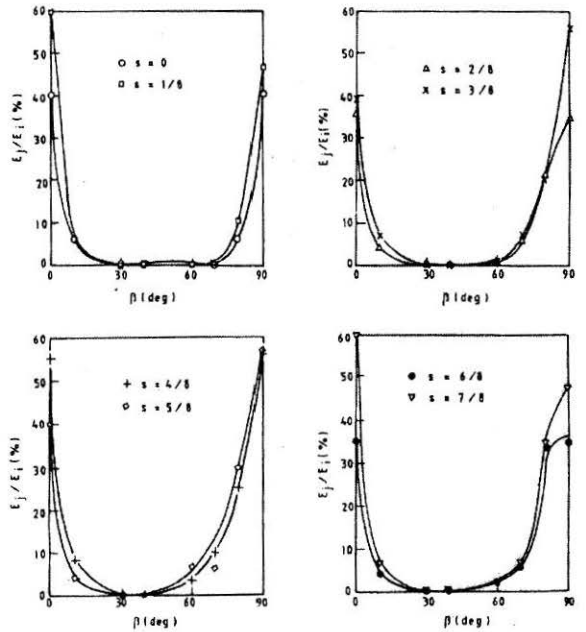

FIGURE 6a : Anisotropy in Tangent Modulus (Type-A Specimens)

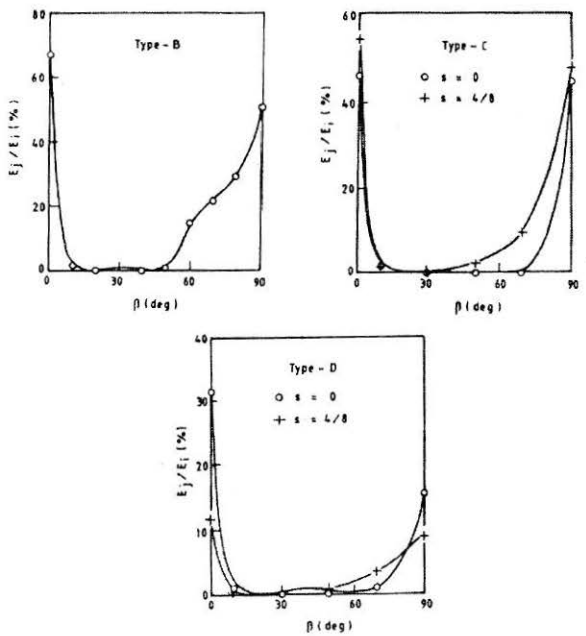

FIGURE 6b : Anisotropy in Tangent Modulus (Type-B, C and D Specimens)

The variation in E_j of the test specimens, against the angle β, is plotted in Figs. 6a and 6b. The modulus in these plots has been shown as a ratio:

$$E_r = \frac{E_j}{E_i} \tag{2}$$

where E_j = tangent modulus of the jointed block mass and

E_i = tangent modulus of the intact material.

For Type-A specimens (s = 0), the value of E_r was about 40% at $\beta = 0°$; it dropped to about 6% at $\beta = 10°$ and 0.2% at $\beta = 30°$. Steep increase took place for $\beta > 70°$. The shape of the anisotropy curve resembles the letter U with a flat base. The mass thus exhibits a highly anisotropic deformational behaviour. Similar to strength, no enhancement in E_j, due to interlocking of the joint set-II was observed for $\beta > 60°$. Also, its extent is low compared to the strength enhancement. The interlocking due to higher stepping, therefore, does make the mass stronger in the range of $\beta > 60°$ but not less deformable to the same extent. There are situations e.g. in mining where higher deformations are allowed, provided the mass is sufficiently strong. For such situations, this aspect may be important. Similar observations were also made for the types C and D specimens.

Failure Modes

The specimens failed in a complex manner and there was always a combination of more than one mechanisms involved in the failure process. It was however possible to identify the most dominating mode initiating the failure of the specimen. Four distinct modes were identified as (i) *splitting*, (ii) *shearing*, (iii) *rotation* and (iv) *sliding*. The typical specimens which failed due to different modes are shown in Fig.7. Elaborations on the four modes of failure are presented in the following:

Splitting

The term splitting implies failure of material due to tensile stresses developed inside it. The failed specimens show large number of minute cracks, roughly vertical in direction and without any sign of shearing. The crushing of the material has also been considered under this category.

Shearing

The specimen fails along one or more shearing planes that are inclined and might pass through the intact material and the pre-existing joints. Signs

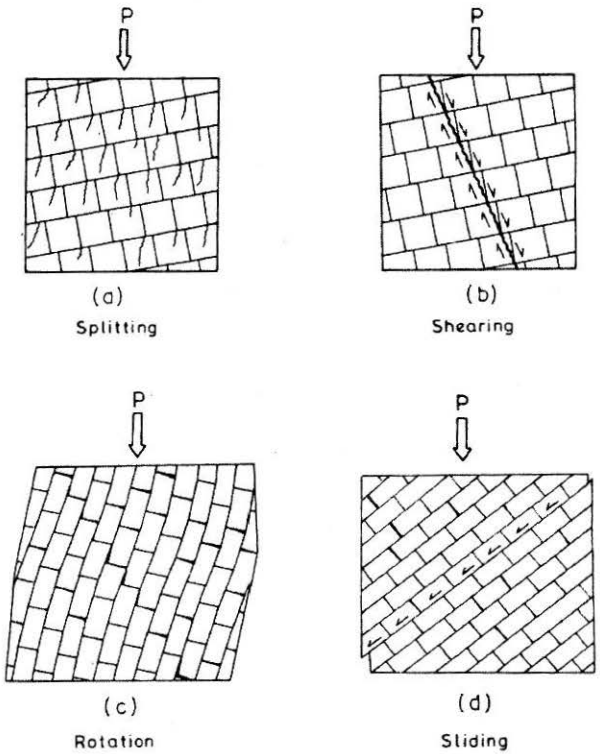

FIGURE 7 : Sketches of Failure Modes

of displacement along the shearing planes are indicated by the specimens. Gouge material is also formed due to shearing. Practically shearing and splitting have been found to occur simultaneously.

Rotation

The rotation of the blocks takes place right from the beginning of the loading of the specimen. Due to friction free end loading system, the specimen as a whole translates and large relative displacement in transverse direction was observed. The elemental blocks forming the specimen generally remain intact.

Sliding

The failure was initiated by sliding on the critically oriented continuous joints. The failure mode is associated with large deformations, stick-slip phenomenon and poorly defined peak in stress-strain curve. At large

deformations, the mode is mostly associated with either rotation or material failure or any other complex combination of the modes.

Observations on Modes of Failure

The summary of failure modes occurring for various combinations of stepping and orientation for Type-A specimens is presented in Table 3. It has been observed that a particular failure mode lies in specific range of orientation of continuous joints and stepping. As discussed earlier, if the continuous joint set is inclined close to the critical orientation $(45° - \phi_m/2)$, the specimen fails due to sliding mode. If interlocking is high due to stepping and joint set-II is close to the critical orientation, shearing and splitting is observed. Rotational failure occurs due to combination of geometry of the block and steep joint inclination. The failure modes observed for Types-B, C and D specimens more or less confirm to these findings. Guidelines are suggested to roughly estimate the probable failure mode of a jointed rock mass under unconfined state in the field. It has been assumed in these guidelines that the mass has two sets of joints effectively governing the behaviour, out of which one is continuous and the other is at low, intermediate or high level of interlocking as per the assessment of the investigator in the field. In case there are more sets of joints, the method of superposition may be employed.

Guidelines For Assessing Failure Modes

i. For $\theta \approx 0$ to $10°$

The failure is likely to occur due to *Splitting* of intact material of blocks.

ii. For $\theta \approx 10°$ to $0.8\,\phi_j$

The mode of failure will depend upon the interlocking conditions and will vary from sliding to splitting, depending upon the combination of interlocking and orientation. In general, for low interlocking, sliding may be assumed and for high interlocking, the mode may be assumed to be shifting towards shearing and then splitting.

For sub horizontal continuous joints ($\approx 10°$), the shifting of failure mode from sliding to shearing is expected to occur if the interlocking is of slightly less than the intermediate level. If the interlocking is very high, the failure mode may be taken as splitting. If the dip of continuous joints is near 20°, the shifting of failure mode from sliding to shearing may be taken near intermediate level of interlocking whereas for joints dipping near $0.8\,\phi_j$, this transition may be taken to occur near high level of interlocking.

TABLE 3a : Summary of Modes of Failure for Type-A Specimens

$\theta°$	Stepping, s							
	0	1/8	2/8	3/8	4/8	5/8	6/8	7/8
0	SHR+ SPL	SHR+ SPL	SPL	SPL	SPL	SPL	SPL	SHR+ SPL
10	ROT	SLD	SHR	SHR	SHR	SHR	SPL	SPL
20	SLD	SLD	SLD	SHR+ SPL	SHR+ SPL	SPL	SPL	SPL+ SHR
30	SLD	SLD	SLD	SLD	SLD+ ROT	SHR	SHR	SHR+ SPL
50	SLD	SLD	SLD	SLD	SLD	SLD	SLD	SLD
60	SLD	SLD	SLD	SLD	SLD	SLD	SLD	SLD
80	ROT	ROT	ROT	ROT	ROT	ROT	ROT	ROT
90	SHR+ SPL	SPL+ SHR	SHR	SHR	SHR	SHR	SHR	SPL+ SHR

SPL: Splitting; SHR: Shearing; ROT: Rotation; SLD: Sliding

TABLE 3b : Summary of Modes of Failure for Types-B, C and D Specimens

$\theta°$	Type-B	Type – C		Type - D	
		s = 0	s = 4/8	s = 0	s = 4/8
0	SPL	SPL	SPL	SPL	SPL
10	SPL	–	–	–	–
20	SPL	SLD	SPL	SLD	SHR
30	SPL	–	–	–	–
40	SLD	SLD	SLD	SLD	SLD
50	SLD	–	–	–	–
60	–	SLD	SLD	ROT	SLD
70	ROT	–	–	–	–
80	ROT	ROT	ROT	ROT	ROT
90	SPL	SPL	SPL	SPL	SPL

iii. For $\theta \approx 0.8\,\phi_j$ to 65°

The mode of failure is expected to be *Sliding* only. Theoretically, the mass should slide down due to its own weight if $\theta > \phi_j$. However the experimental observations (Singh, 1997) indicate that the mass fails due to its own weight if it has a single joint set only. If there are more than one joint set, the mass does not fail ultimately, rather deforms to some extent and becomes stable. It is due to small amount of rotation of blocks due to which the corners of the blocks introduce some interlocking and create apparent cohesion in the mass. The net result is that the mass does have some strength due to the apparent cohesion.

iv. For $\theta \approx 65°$ to 75°

The mode of failure shifts from *Sliding* at ($\theta = 65°$) to *Rotation* of blocks (at $\theta = 75°$).

v. For $\theta \approx 75°$ to 85°

The mass is likely to fail due to *Rotation* of blocks only. Geometry of the blocks will be an important parameter governing the engineering behaviour of the mass.

vi. For $\theta \approx 85°$ to 90°

The failure mode shifts for *Rotation* at $\theta = 85°$ to *Shearing* at $\theta = 90°$. It may be noted that steep changes take place in the response of the mass in this range of orientation.

The mode of failure may be modified depending upon the restraining conditions on the boundaries of the mass even though it may be under uniaxial stress state. For example, the two sidewalls in an underground or open excavation may have same condition of joints. But on one side, the blocks will be free to slide down, (say for $\theta \approx 60°$) whereas on the other side, they will be restrained. Accordingly, the mode of failure on the second side will have to be modified to shearing or splitting.

It may also be noted that the stepping in the present investigation has been an indirect measure of interlocking level of the jointed mass. In field, these ideal conditions of stepping do not occur. However, based on the conditions of joints and the previous displacement history, the level of interlocking may be assessed as low, medium or high and correspondingly these conditions will roughly be equivalent to s = 0, 4/8 and 7/8 respectively. One can assess the boundaries within which the mass is expected to behave by assigning the probable mode of failure for a specific interlocking condition.

The interlocking conditions of jointed rock mass also change with time. These changes may result from opening of cracks, loosening of the rock mass due to some external reasons such as stress relief, earthquake forces, seasonal variations of water level, freezing of water in the cracks and creep of filling material (Ladanyi and Archambault, 1970). The interlocking may decrease up to considerable degree. The influence of change in the interlocking conditions on the strength behaviour can be studied by assigning the appropriate change in the mode of failure.

Relation Between Strength, Tangent Modulus and Failure Strain

Results obtained from the present experimental investigations were plotted on Deere-Miller (1966) charts (Figs.8 to 12) according to different modes of failure. The location of the jointed specimen on these charts, is represented by its strength and tangent modulus on log-log scale. The position of the intact model material is shown as 'I'. A best fitting line is plotted through all the points. It is interesting to observe that the best fitting line starts from the intact rock position I and points representing the position of jointed block mass on the classification chart lie near this best fitting line. It has been inferred that if an intact rock is intersected by joints, its strength

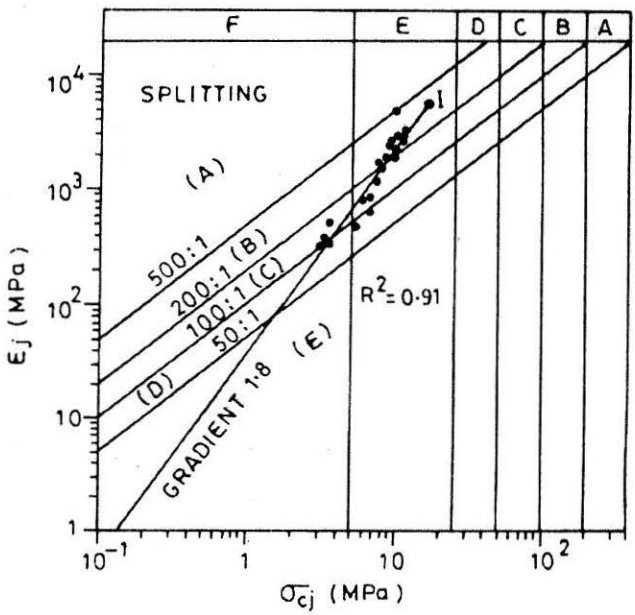

FIGURE 8 : Modulus vs. Strength Values for Splitting Mode of Failure (Chart as per Ramamurthy and Arora, 1993)

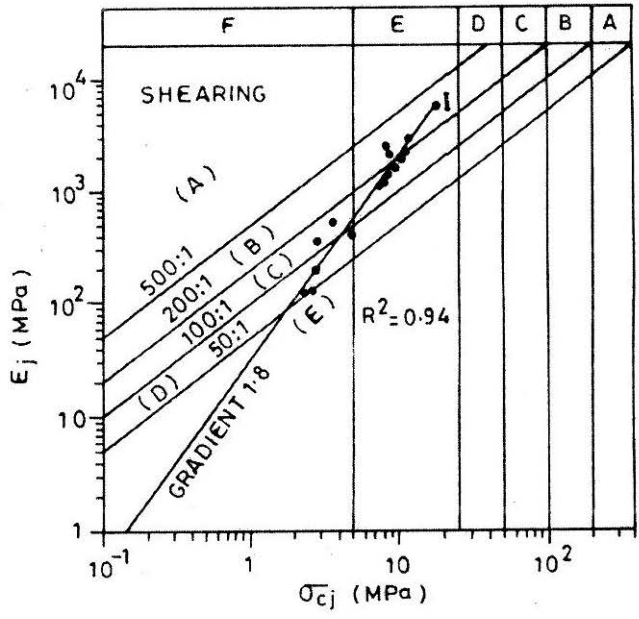

FIGURE 9 : Modulus vs. Strength Values for Shearing Mode of Failure (Chart as per Ramamurthy and Arora, 1993)

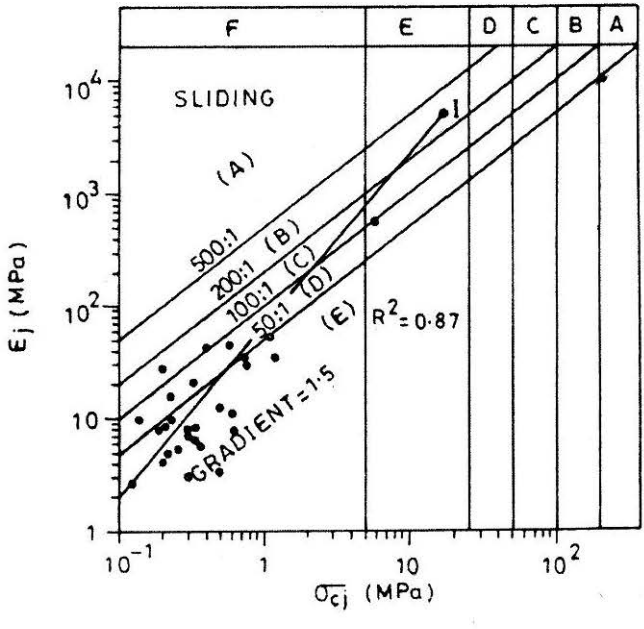

FIGURE 10 : Modulus vs. Strength Values for Sliding Mode of Failure (Chart as per Ramamurthy and Arora, 1993)

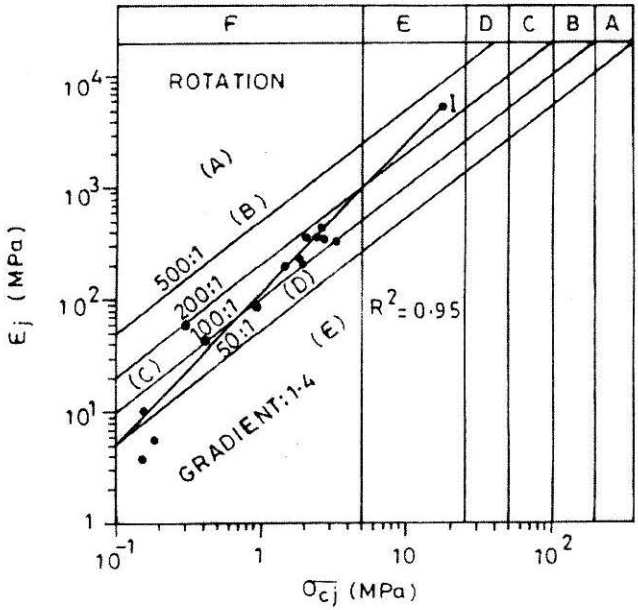

FIGURE 11 : Modulus vs. Strength Values for Rotation Mode of Failure (Chart as per Ramamurthy and Arora, 1993)

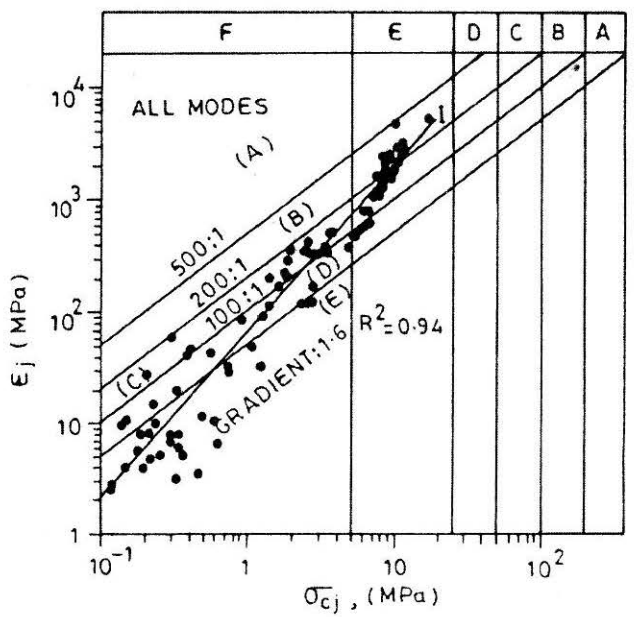

FIGURE 12 : Modulus vs. Strength Values for All Modes of Failure (Chart as per Ramamurthy and Arora, 1993)

and tangent modulus reduce in such a manner that its position on Deere-Miller classification chart moves on an empirical line that has a specific gradient which depends on the failure mode. The values of gradient of this empirical line for splitting, shearing, sliding and rotational modes has been observed as 1.8, 1.8, 1.5 and 1.4 respectively (Figs.8 to 11). From a combined plot for all the modes, an average value of the gradient of the empirical line has been obtained as 1.6 (Fig.12). The position of jointed mass on the classification chart moves along the empirical line as degree of jointing increases and the rock mass is more and more inferior in strength and tangent modulus. The gradient of this empirical line may be used to develop a correlation between σ_{cj}, E_j, σ_{ci} and E_i as follows:

$$\text{Gradient of the line} = \frac{\log E_i - \log E_j}{\log \sigma_{ci} - \log \sigma_{cj}} = \frac{\log\left(\frac{E_j}{E_i}\right)}{\log\left(\frac{\sigma_{cj}}{\sigma_{ci}}\right)}$$

$$\Rightarrow \frac{\sigma_{cj}}{\sigma_{ci}} = \left[\frac{E_j}{E_i}\right]^{1/\text{Gradient}} \quad \text{or} \tag{3}$$

$$SRF = (MRF)^{ng} \tag{4}$$

where SRF = Strength Reduction Factor = σ_{cj}/σ_{ci}

MRF = Modulus Reduction Factor = E_j/E_i

ng = Index = $\dfrac{1}{\text{Gradient of the empirical line}}$

= 0.56 for Splitting and Shearing

= 0.66 for Sliding

= 0.72 for Rotation

= 0.63 Average for all modes.

E_i and E_j = tangent moduli of the intact rock and jointed mass respectively;

σ_{ci} and σ_{cj} = uniaxial compressive strength of intact and jointed rock respectively.

Equation (3) indicates that correlation exists between strength and the modulus of jointed block mass through the intact rock properties. The intact rock properties, namely, σ_{ci} and E_i are generally available from laboratory tests. The value of E_j may be obtained from field tests e.g. Uniaxial Jacking Test (IS:7317-1974). The failure mode may be assigned on basis of the guidelines suggested earlier. The value of uniaxial compressive strength of rock mass may therefore be estimated through Eqn.(3).

The modulus ratio of the jointed mass is a measure of the failure strain and is defined as:

$$M_{rj} = \frac{E_j}{\sigma_{cj}} \tag{5}$$

For a linear elastic body, M_{rj} will be exactly equal to the inverse of failure strain. The axial stress-strain curves obtained in the present investigation were non-linear and S-shaped, having their initial part concave upward followed by linear portion and then third part concave downward near failure. To get the correlation, failure strain was plotted against the modulus ratio (Fig.13) for all the specimens tested in the present study. Following correlation has been obtained for failure strain:

$$\varepsilon_{aj} \approx 82.5\left(M_{rj}\right)^{-0.85} = 82.5\left[\frac{E_j}{\sigma_{cj}}\right]^{-0.85} \% \tag{6}$$

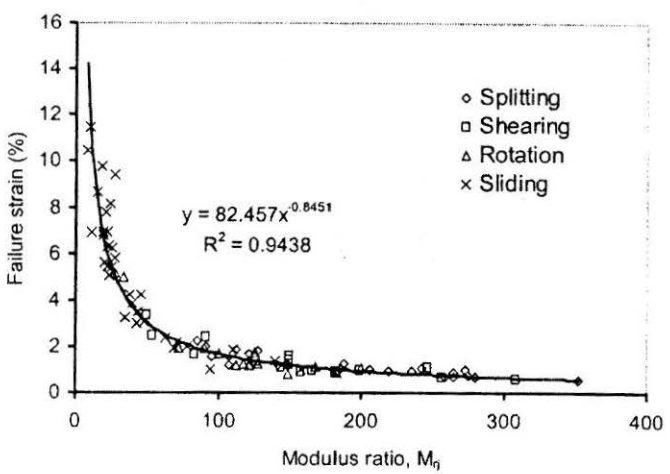

FIGURE 13 : Variation of Axial Failure Strain with Modulus Ratio

To demonstrate the applicability of the above relationships to field problems, some case studies were taken up. The designers often require the secant modulus of deformation of jointed mass. Mehrotra (1992) has reported results of uniaxial jacking tests (IS:7317-1974) along with laboratory tests for rock masses in some projects in the lower Himalayas. The results on modulus of intact rock (E_i) and modulus of elasticity of jointed mass ($E_j = E_e$) are presented in Table 4. To check the applicability of the correlations suggested above, the secant modulus of deformation was computed and compared with field test results. Following steps are proposed to compute the modulus of deformation E_d:

i. Compute MRF = E_j/E_i, where $E_j = E_e$ = modulus of elasticity obtained from uniaxial jacking test.

ii. Obtain $\sigma_{cj} = \sigma_{ci}\,(MRF)^{ng}$ where index, ng is taken 0.63 (average for all modes) as no sufficient information was available from Mehrotra (1992) to assess the failure mode.

iii. Obtain modulus ratio $M_{rj} = E_e/\sigma_{cj}$.

iv. Compute failure strain $\varepsilon_{aj} = 82.5\left(M_{rj}\right)^{-0.85}$.

v. Compute modulus of deformation $E_d = \sigma_{cj}/\varepsilon_{aj}$.

The computations are also shown in Table 4 and the computed values of E_d are compared with the values observed in the field (Fig.14). A close agreement of computed and predicted values of the modulus of deformation, E_d validates the applicability of the correlations suggested above.

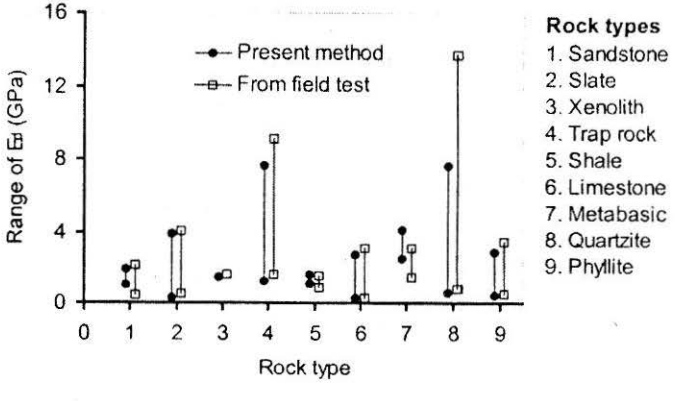

FIGURE 14 : Comparison of Predicted and Field Values of E_d

TABLE 4 : Results of Laboratory and Field Tests for Various Rock Types (after Mehrotra, 1992)

Sl. No.	Rock type	σ_{ci} (MPa)	E_i (GPa)	Field E_e (GPa)	Field E_d (GPa)	MRF = E_e/E_i	$\sigma_{cj} = \sigma_{ci}(MRF)^{0.63}$ (MPa)	$M_{rj} = E_e/\sigma_{cj}$	$\varepsilon_{aj} = 82.5(M_{rj})^{-0.85}$ (%)	Predicted E_d $\sigma_{cj}/\varepsilon_{aj}$ (GPa)
1.	Sandstone	32.00 – 75.00	6.76	1.75 – 2.90	0.44 – 2.10	0.259 – 0.429	13.66 – 44.00	128.11 – 65.91	1:33 – 2.35	1.02 – 1.88
2.	Slate	1.00 – 38.00	20.00	0.98 – 7.80	0.49 – 4.04	0.049 – 0.39	0.15 – 20.99	65.33 – 371.6	0.05 – 0.54	0.32 – 3.89
3.	Xenolith	21.00	14.74	2.95	1.58	0.200	7.99	369.21	0.54	1.47
4.	Trap rock	98.00 – 196.50	12.35 36.43	1.98 – 13.00	1.60 – 9.12	0.160 – 0.357	30.93 – 102.67	64.00 – 126.62	2.40 – 1.35	1.28 – 7.62
5.	Shale	16.80 – 37.00	10.80	2.22 – 2.95	0.90 – 1.57	0.206 – 0.730	6.20 – 16.34	358.06 – 180.54	0.56 – 1.00	1.11 – 1.64
6.	Limestone	21.00 – 49.00	11.80	0.55 – 4.80	0.26 – 3.08	0.047 – 0.407	3.03 – 27.66	181.52 – 173.54	0.99 – 1.03	0.31 – 2.68
7.	Metabasic	70.90 – 104.00	22.40	4.38 – 7.11	1.45 – 3.08	0.196 – 0.317	26.41 – 50.47	165.85 – 140.88	1.07 – 1.23	2.47 – 4.10
8.	Quartzite	67.00 – 128.00	28.25 – 49.80	0.98 – 14.37	0.84 – 13.70	0.035 – 0.289	8.06 – 58.50	121.59 – 245.64	1.39 – 0.77	0.58 – 7.63
9.	Phyllite	38.00 – 133.00	6.68 – 7.07	0.73 – 4.13	0.54 – 3.48	0.109 – 0.584	9.42 – 94.79	77.49 – 43.57	2.04 – 3.34	0.46 – 2.84

Prediction of Strength and Modulus through Joint Factor

The concept of Joint Factor suggested by Ramamurthy and co-workers (Ramamurthy, 1993; Ramamurthy and Arora, 1994) and modified by Singh (1997) and Singh et al. (2002) may also be used to assess the strength and tangent modulus of jointed rock masses. The Joint Factor is a weakness coefficient that indicates the effect of joints on the intact rock behaviour. The Joint Factor J_f, is defined as:

$$J_f = \frac{J_n}{n\,r} \tag{7}$$

where J_n = number of joints or potential failure surfaces /m depth in the direction of loading;

n = critical joint inclination parameter as given in Table 5 and

r = sliding joint strength parameter = $\tan\phi_j$; where ϕ_j is the friction angle along the critical joint at sufficiently low normal stress so that the initial roughness of the surface is reflected through this value.

The Joint Factor was computed for the specimens tested during this study. For splitting mode, J_n was computed by counting potential failure surfaces (1) and (2) shown in Fig.15(a). For shearing and rotational mode, the potential failure surfaces (1), (2-A) and (2-B) as shown in the Fig.15(b)

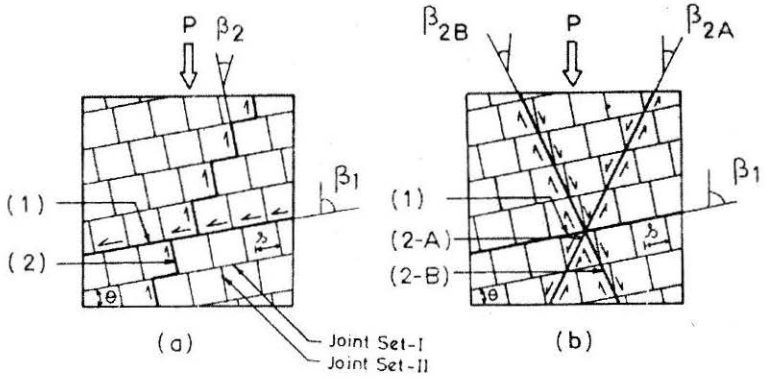

FIGURE 15 : Potential Failure Surfaces for Stepped Joints

TABLE 5 : Joint Inclination Parameter, n (Ramamurthy, 1993)

Orientation of joint, $\beta°$	Inclination Parameter, n	Orientation of joint $\beta°$	Inclination Parameter, n
0	0.810	50	0.306
10	0.460	60	0.465
20	0.105	70	0.634
30	0.046	80	0.814
40	0.071	90	1.000

β = Angle between the joint plane and direction of stress

were considered. For specimens, which failed due to sliding, only the surface (1) as shown in Fig.15(a) was considered. The results on strength and tangent modulus for the specimens which failed due to various failure modes and corresponding values of J_f are presented in Tables 6 to 9. The results have also been presented in Figs.16 and 17 so to observe the effect of Joint Factor on the strength and deformability of the mass. The strength and modulus values in these plots were non-dimensionalised by dividing them by respective intact rock property. It has been observed that both the properties decrease exponentially with increasing Joint Factor. Correlations of σ_{cj} and E_j with J_f for different failure modes have been obtained by best fitting curves and are given below:

Splitting/Shearing

$$\left.\begin{aligned} \sigma_{cj} &= \sigma_{ci}\exp(-0.012J_f) \\ E_j &= E_i\exp(-0.020J_f) \end{aligned}\right\} \quad (8)$$

Sliding

$$\left.\begin{aligned} \sigma_{cj} &= \sigma_{ci}\exp(-0.018J_f) \\ E_j &= E_i\exp(-0.035J_f) \end{aligned}\right\} \quad (9)$$

Rotation

$$\left.\begin{aligned} \sigma_{cj} &= \sigma_{ci}\exp(-0.025J_f) \\ E_j &= E_i\exp(-0.040J_f) \end{aligned}\right\} \quad (10)$$

It may be noted that almost same correlations were obtained for

TABLE 6 : Values of J_f, σ_{cr} and E_r for Splitting Mode of Failure

Specimen Type	θ^o	s	J_f	σ_{cr}	E_r
A	00	2/8	43.1	0.5985	0.3470
A	00	3/8	43.1	0.6634	0.5670
A	00	4/8	43.3	0.6696	0.5582
A	10	6/8	59.3	0.5539	0.3392
A	10	7/8	59.5	0.5815	0.3482
A	20	5/8	510.1	0.1938	0.0630
A	20	6/8	606.5	0.1909	0.0630
A	20	7/8	402.4	0.1988	0.0709
A	20	1/8	17.1	0.6923	0.6048
B	00	-	44.2	0.6483	0.5039
B	10	-	61.9	0.4808	0.2864
B	20	-	81.0	0.4463	0.2160
B	30	-	109.0	0.3697	0.1512
B	90	-	10.4	0.6420	0.6737
C	00	0	44.2	0.5796	0.4500
C	90	0	25.0	0.6226	0.4610
C	00	4/8	42.8	0.5558	0.4800
C	20	4/8	103.8	0.2188	0.0975
C	90	4/8	33.76	0.6498	0.5425
D	00	0	91.2	0.3766	0.1551
D	90	0	42.8	0.4508	0.3149
D	00	4/8	94.7	0.3205	0.0886
D	90	4/8	52.0	0.4014	0.1181

splitting and *shearing* modes. The J_f concept may also be used to assess the strength and tangent modulus of a rock mass in the field. The probable mode of failure may be assigned from the guidelines suggested previously and the strength and tangent modulus may be computed by using expressions suggested in Eqns.(8), (9) and (10).

Conclusions

Based on the experimental investigation carried out in the present study, the following conclusions are derived:

TABLE 7 : Values of J_r, σ_{cr} and E_r for Shearing Mode of Failure

Specimen Type	θ^o	s	J_r	σ_{cr}	E_r
A	00	0	42.8	0.6812	0.4040
A	00	1/8	43.3	0.5508	0.4699
A	10	2/8	61.5	0.4214	0.2122
A	10	3/8	70.0	0.4273	0.2010
A	10	4/8	72.0	0.4938	0.2511
A	10	5/8	59.0	0.5452	0.2953
A	20	3/8	152.0	0.2812	0.0741
A	20	4/8	188.9	0.2055	0.1008
A	30	5/8	166.0	0.1462	0.0667
A	30	6/8	256.5	0.1295	0.0236
A	30	7/8	533.0	0.1392	0.0233
A	90	2/8	51.3	0.6039	0.3535
A	90	3/8	50.9	0.5856	0.3976
A	90	4/8	52.0	0.6351	0.5498
D	20	4/8	455.6	0.1710	0.0349

TABLE 8 : Values of J_r, σ_{cr} and E_r for Sliding Mode of Failure

Specimen Type	θ^o	s	J_r	σ_{cr}	E_r
A	10	1/8	63	0.6812	0.1054
A	20	0	243	0.5508	0.0039
A	20	1/8	81	0.0115	0.0053
A	20	2/8	106	0.0268	0.0021
A	30	1/8	110	18.21	0.0084
A	30	3/8	122	0.0394	0.0061
A	30	4/8	109	0.0870	0.0336
A	50	0	485	0.0402	0.0054
A	50	1/8	485	0.0265	0.0007
A	50	2/8	467	0.0309	0.0006
A	50	3/8	476	0.0074	0.0005
A	50	4/8	495	0.0870	0.0005
A	50	5/8	476	0.0144	0.0010
A	50	6/8	479	0.0108	0.0008
A	50	7/8	479	0.0148	0.0010
A	60	1/8	739	0.0170	0.0015
A	60	2/8	749	0.0124	0.0009
A	60	3/8	739	0.0121	0.0016

TABLE 8 : Continued

Specimen Type	θ°	s	J_f	σ_{cr}	E_r
A	60	4/8	735	0.0185	0.0012
A	60	5/8	735	0.0185	0.0012
A	60	6/8	735	0.0182	0.0016
A	60	7/8	744	0.0190	0.0010
B	40	-	137	0.0683	0.0064
B	50	-	476	0.0364	0.0013
C	20	0	160	0.0082	0.0019
C	40	0	355	0.0281	0.0023
C	40	4/8	137	0.1691	0.0236
C	60	0	725	0.0120	0.0015
C	60	4/8	739	0.0137	0.0030
D	20	0	245	0.0248	0.0081
D	40	0	485	0.0185	0.0013
D	40	4/8	282	0.0542	0.0096
D	60	4/8	1302	0.0124	0.0019

TABLE 9 : Values of J_f, σ_{cr} and E_r for Rotational Mode of Failure

Specimen Type	θ°	s	J_f	σ_{cr}	E_r
A	10	0	59.3	0.1956	0.0616
A	80	1/8	126.0	0.1549	0.0636
A	80	2/8	109.9	0.0865	0.0391
A	80	3/8	105.7	0.1204	0.0681
A	80	4/8	135.3	0.1428	0.0810
A	80	5/8	189.5	0.1039	0.0419
A	80	6/8	336.9	0.1023	0.0399
A	80	7/8	620.5	0.1245	0.0676
B	70	-	242.9	0.0093	0.0007
B	80	-	36.5	0.0183	0.0116
C	80	0	41.0	0.0507	0.0187
C	80	4/8	237.7	0.0571	0.0158
D	60	0	1123.4	0.0104	0.0011
D	80	0	62.7	0.0260	0.0090
D	80	4/8	745.2	0.0080	0.0020

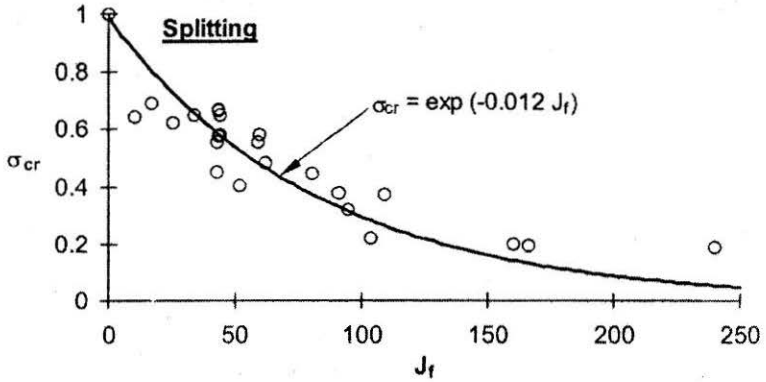

FIGURE 16a : Variation of σ_{cr} with J_f for Splitting Mode of Failure

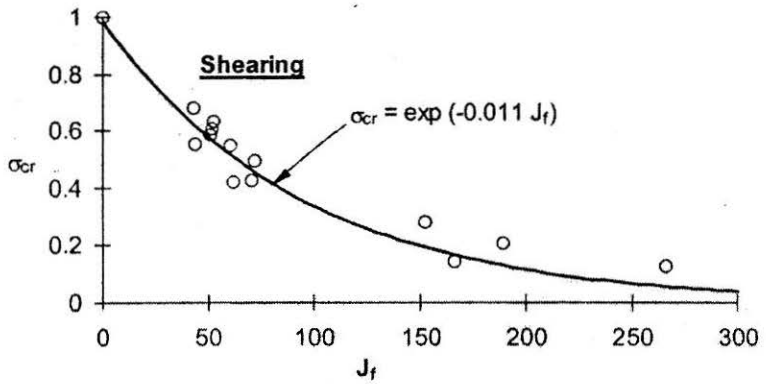

FIGURE 16b : Variation of σ_{cr} with J_f for Shearing Mode of Failure

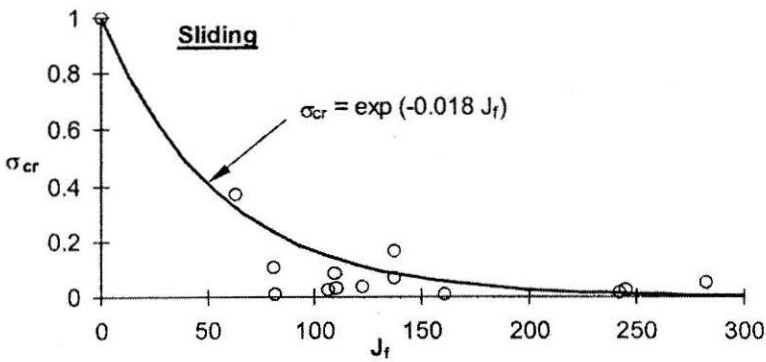

FIGURE 16c : Variation of σ_{cr} with J_f for Sliding Mode of Failure

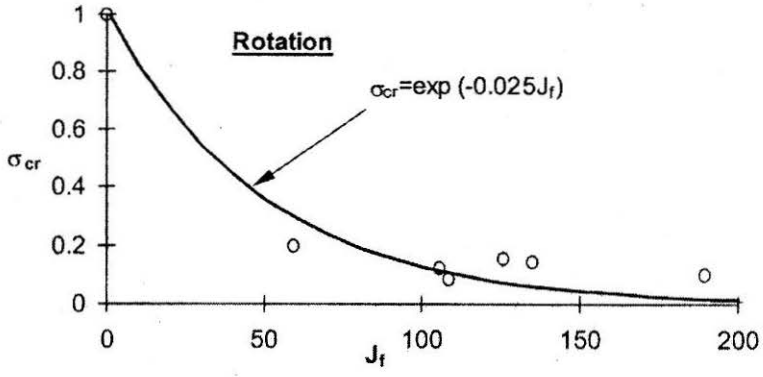

FIGURE 16d : Variation of σ_{cr} with J_f for Rotational Mode of Failure

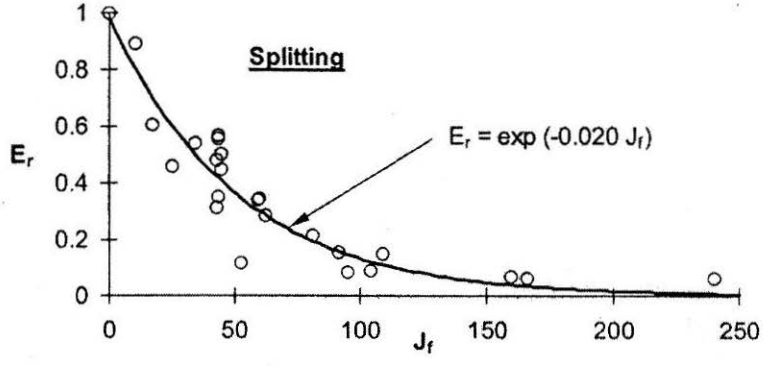

FIGURE 17a : Variation of E_r with J_f for Splitting Mode of Failure

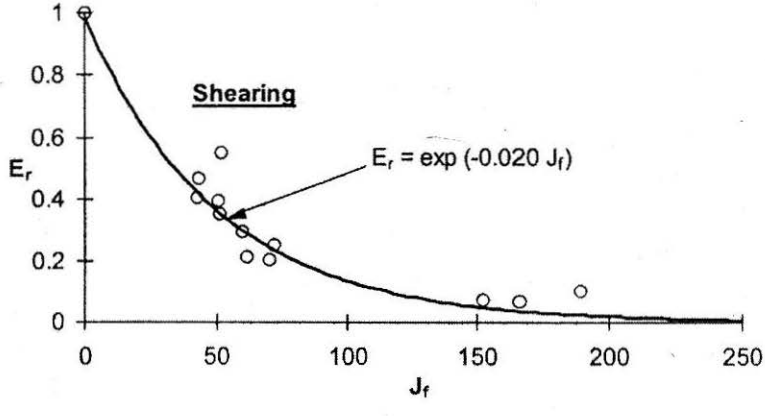

FIGURE 17b : Variation of E_r with J_f for Shearing Mode of Failure

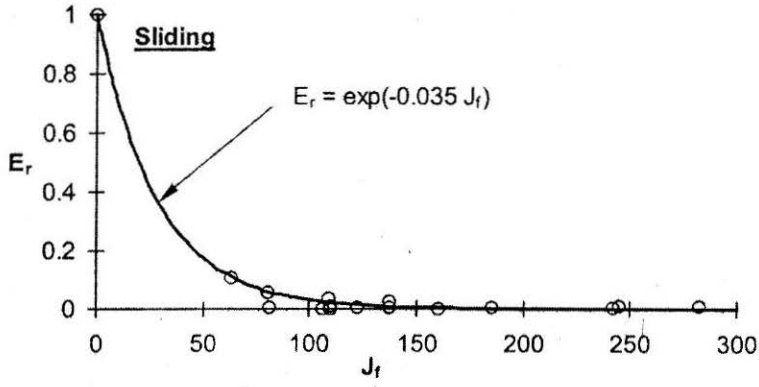

FIGURE 17c : Variation of E_r with J_f for Sliding Mode of Failure

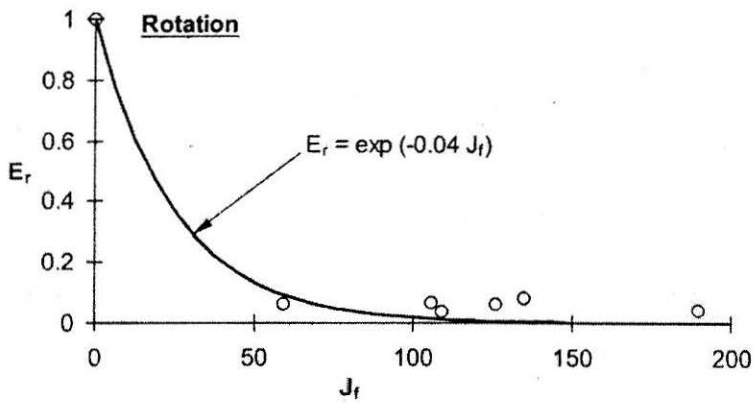

FIGURE 17d : Variation of E_r with J_f for Rotational Mode of Failure

i. The jointed mass behaves highly anisotropically in strength and deformational behaviour. The anisotropy curves obtained are U shaped with flat base.

ii. A jointed mass under uniaxial loading condition may fail due to splitting, shearing, rotation or shearing depending upon the inclination and interlocking of the joints. The failure mode is governed by the fact, that, whether the continuous joints are aligned along or across the potential failure planes (inclined at $\beta \approx 45° - \phi_m/2$). Guidelines have been suggested to assess the probable failure mode based on experimental observations.

iii. An empirical line may be drawn on Deere-Miller classification chart, starting from intact rock position to indicate the degree of jointing of the mass. For splitting, shearing, sliding and rotation modes, the gradient of this empirical line on log-log scale is 1.8, 1.8, 1.5 and 1.4 respectively. From the combined data for all the modes, the average gradient has been obtained as 1.6.

iv. The rock mass strength in the field may be obtained by computing the Strength Reduction factor as SRF = $(MRP)^{ng}$, where ng is an index and its value is 0.56, 0.56, 0.66, 0.72 and 0.63 for splitting, shearing, sliding, rotation and combined modes respectively.

v. The failure strain of a jointed mass varies non-linearly with modulus ratio and may be computed as $\varepsilon_{aj} \approx 82.5(M_{rj})^{-0.85}$.

vi. The strength and tangent modulus of the jointed block mass are found to be failure mode dependent and may be assessed through Joint Factor concept. The correlations for computing these properties for various failure modes have been suggested.

References

ABDULLAH, H. and DHAWAN, A.K. (2003) : "Scatte- in Rock Engineering", *Proc. IGC-2003 - Geotechnical Engineering for Infrastructural Development,* Dec. 18-20, Roorkee, India, 543-550.

ARORA, V.K. (1987) : "Strength and Deformational Behaviour of Jointed Rocks", *Ph.D. Thesis*, IIT Delhi, India.

BAOSHU, G., HUOYAO, X. and HANMIN, W. (1986) : "An Experimental Study on the Strength of Jointed Rock Mass", *Proc. Int. Symp. on Engineering in Complex Rock Formations*, 3-7 Nov, Beijing, China, 190-198.

BARTON, N.R., LIEN, R. and LUNDE, J. (1974) : "Engineering Classification of Rock Masses for the Design of Tunnel Support". *Rock Mech.* 6(4), 189-239.

BIENIAWSKI, Z.T. (1973) : "Engineering Classification of Jointed Rock Masses", *Trans. S. Afr. Inst. Civ. Engrs,* 15, 335-344.

BIENIAWSKI, Z.T. (1989) : *Engineering Rock Mass Classifications*, New York: Wiley.

BROWN, E.T. (1970a) : "Strength of Models of Rock with Intermittent Joints", *Jl. of Soil Mech. & Found. Div.*, Proc. ASCE, 96(SM6), 1935-1949.

BROWN, E.T. (1970b) : "Modes of Failure in Jointed Rock Masses", *Proc. of the Second Cong. of ISRM,* Belgrade, Vol-II, 293-298.

BROWN, E.T. and TROLLOPE, D.H. (1970) : "Strength of a Model of Jointed Rock", *Jl. of Soil Mech. & Found. Div.*, Proc. ASCE, 96(SM2), 685-704.

DEERE, D.U. and MILLER, R.P. (1966) : "Engineering Classification and Index

Properties for Intact Rock", *Technical Report No. AFNL-TR-65-116.* Air Force Weapons Laboratory, New Mexico.

EINSTEIN, H.H. and HIRSCHFELD, R.C. (1973) : "Model Studies on Mechanics of Jointed Rock", *Jl. of Soil Mech. & Found. Div.* Proc. ASCE, 90, 229-248.

GOLDSTEIN, M. GOOSEV. B., PYROGOVSKY, N., TULINOV, R. and TUROVSKAYA, A. (1966) : "Investigation of Mechanical Properties of Cracked Rock", *Proc Ist Cong., Int. Soc. Rock. Mech.*, Lisbon, 1, 521-524.

HAYASHI, M. (1966) : "Strength and Dialatancy of Brittle Jointed Mass - The Extreme Value Stochastic and Anisotropic Failure Mechanism", *Proc Ist Cong. ISRM,* Lisbon, 1, 295-302.

HOEK, E. (2000) : *Practical Rock Engineering*, 2000 Edition, http://www.rocscience.com/roc/Hoek/Hoeknotes2000.htm.

IS:7317 (1974) : "Code of Practice for Uniaxial Jacking Test for Modulus of Deformation of Rocks".

ISRM (1981) : "*Rock Characterization, Testing and Monitoring*", ISRM Suggested Methods, Brown E.T. (ed.), Pergamon Press, 211 pages.

LADANYI, B. and ARCHAMBAULT, G. (1970) : "Simulation of Shear Behaviour of a Jointed Rock Mass", *Rock Mechanics: Theory and Practice*, Proc. 11th Symp. Rock Mech., Berkeley, California, 105-125.

LADANYI, B. and ARCHAMBAULT, G. (1972) : "Evaluation of Shear Strength of a Jointed Rock Mass", *Proc. 24th Int. Geological Congress,* Montreal, Section 13D, 249-270.

LAMA, R.D. (1974) : "The Uniaxial Compressive Strength of Jointed Rock", Prof. L. Müller Festschrift, *Inst. Soil Mech. & Rock Mech.*, Univ. Karlsruhe, Karlsruhe, 67-77.

MEHROTRA, V.K. (1992) : "Estimation of Engineering Parameters of Rock Mass", *Ph. D Thesis*, University of Roorkee, Roorkee, India.

RAMAMURTHY, T. (1993) : "Strength and Modulus Response of Anisotropic Rocks", Chapter 13, *Comprehensive Rock Engg.*, Vol 1, Pergamon Press, U.K., 313-329.

RAMAMURTHY, T. and ARORA, V.K. (1993) : "A Classification for Intact and Jointed Rocks", *Geotechnical Engineering of Hard Soils-Soft Rocks*, Angnostopoulos et al. (eds.), 235-242.

RAMAMURTHY, T. and ARORA, V.K. (1994) : "Strength Prediction for Jointed Rocks in Confined and Unconfined States", *Int. J. Rock Mech. Min. Sci. & Geomech. Abstr.*, 31(1), 9-22.

ROY, N. (1993) : "Engineering Behaviour of Rock Masses Through Study of Jointed Models.", *Ph.D. Thesis*, IIT Delhi, India.

SINGH, J., RAMAMURTHY, T. and RAO, G.V. (1989) : "Strength Anisotropies in Rocks", *Indian Geotechnical Journal*, 19(2), 147-166.

SINGH, M. (1997) : "Engineering Behaviour of Jointed Model Materials", *Ph.D. Thesis*, IIT, New Delhi, INDIA.

SINGH, M., RAO, K.S. and RAMAMURTHY, T. (2002) : "Strength and Deformational Behaviour of a Jointed Rock Mass", *Int. Jl. Rock Mech. Rock Engg.*, 35 (1), 45-64.

WALKER, P.F. (1971) : "The Shearing Behaviour of Block Jointed Rock Model", *Ph.D. Thesis*, Queens Univ., Belfast, Northern Ireland.

WICKHAM, G.E., TIEDEMANN, H.R. and SKINNER, E.H. (1972) : "Support Determination Based on Geologic Predictions", In *Proc. North American Rapid Excav. Tunnelling Conf.*, Chicago, (eds K.S. Lane and L.A. Garfield), 43-64, New York: Soc. Min. Engrs, Am. Inst. Min. Metall. Petrolm Engrs.

XU, S., GRASSO, P., and BOHLOULI, M. (2003) : "The Role of Ground Improvement in Bridging the Gap Between a Discontinuous Reality and a Continuous Model", *Proc. of the Sixth International Conf. on Analysis of Discontinuous Deformation,* 5-8, October, 2003, Tromdheim, Norway, 223-235.

YANG, Z.Y. and HUANG, T.H. (1995) : "Effect of Joint Sets on the Anisotropic Strength of Rock Masses", *Proc. 8th Cong. ISRM*, Japan, 367-370.

Notations

β	=	Orientation of joint plane with loading direction
θ	=	Inclination of joint set–I with the horizontal
ε_{aj}	=	Failure strain of the jointed mass
σ_{ci}	=	UCS of intact model material
σ_{cj}	=	UCS of jointed block mass
σ_{cr}	=	Strength ratio = σ_{cj}/σ_{ci}
ϕ_j	=	Friction angle along the joints
ϕ_m	=	Friction angle of jointed mass
E_d	=	Modulus of deformation of rock mass in the field
E_i	=	Tangent modulus of intact rock
E_j	=	Tangent modulus of jointed block mass
E_r	=	E_j/E_i
J_f	=	Joint Factor
J_n	=	Number of joints or potential failure surfaces /m depth in the direction of loading
MRF	=	Modulus Reduction Factor = E_j/E_i
M_{rj}	=	Modulus ratio = E_j/σ_{cj}
n	=	Critical joint inclination parameter

ng = An index

r = Sliding joint strength parameter = tan ϕ_j

s = Stepping

SRF = Strength Reduction Factor = σ_{cj}/σ_{ci}

UCS = Uniaxial compressive strength